Building and Environment 47 (2012) 126–137

Contents lists available at ScienceDirect

Building and Environment

journal homepage: www.elsevier.com/locate/buildenv

Analytical procedures for estimating airflow rates in ventilated, screened wall systems (VSWS)

Danko Davidovic [a,*], Joseph Piñon [a], Eric F.P. Burnett [b,c], Jelena Srebric [c]

[a] Building Technology Group, Simpson Gumpertz and Heger Inc., Waltham, MA 02453, United States
[b] Department of Civil & Environmental Engineering, The Pennsylvania State University, University Park, PA, United States
[c] Department of Architectural Engineering, The Pennsylvania State University, University Park, PA, United States

ARTICLE INFO

Article history:
Received 5 November 2010
Received in revised form
7 March 2011
Accepted 1 April 2011

Keywords:
Ventilated and screened wall system (VSWS)
Natural ventilation
Volumetric flow rate
Pressure loss characteristics
Local pressure loss coefficients

ABSTRACT

The wetting, storage and drying of moisture is a serious concern in the overall performance of exterior wall systems. Prediction of moisture transport and moisture removal within wall enclosures plays a key role in the design of exterior wall systems. The convective drying potential in ventilated and screened wall systems (VSWS) is directly proportional to the available ventilation flow rate of the air through the vents in the walls. The main goal of this study was to determine the most appropriate analytical equations for predicting ventilation flow rates within VSWS and to provide a solid foundation for estimating convective drying potential.

The equations currently available in the ASHRAE literature are primarily intended for mechanical system applications and are not well suited for estimates of convective drying potential in wall systems, mainly due to the extremely low velocities and the unique geometry of VSWS when compared to mechanical systems. Other literature sources were also reviewed for the evaluation of pressure losses in systems with low airflow rates. The pressure losses due to friction at the walls of the ventilated chamber were beyond the scope of this paper. Under most circumstances, the major contribution to pressure losses in VSWS occurs at the inlet and outlet vent openings. A list of the empirical/analytical equations recommended for use in evaluating natural ventilation flow characteristics within VSWS is also provided. The recommended equations provide a solid theoretical background for validation against the laboratory and field results obtained in the ASHRAE Research Project RP-1091.

© 2011 Elsevier Ltd. All rights reserved.

1. Introduction

High moisture levels in buildings raise two major concerns: the risk of harmful effects on human health and the risk of physical damage. Moisture control across and within a building enclosure is of great importance to the performance of ventilated and screened wall systems (VSWS) under real operating conditions. Satisfactory performance of these wall systems can be achieved with a better understanding of the nature and characteristics of the wetting, storage, and drying processes. Mathematical modeling of these processes may improve current moisture control strategies and permit more accurate quantification of the potential for removing moisture within the VSWS by means of convective drying. The ventilation flow rate of the air through the system is one of the most significant variables affecting the convective drying process. Hence the most relevant parameters affecting the convective drying process need to be studied in more detail.

The natural ventilation process in ventilated wall systems is governed by two driving forces: wind pressure and natural buoyancy (stack effect). Difficulties arise, however, from the stochastic nature of both driving forces, with less uncertainty associated with characterizing the stack effect. In common HVAC applications the flow rate of working medium is usually prescribed in advance as a characteristic of the system and is a carefully controlled parameter in system operation. However, the airflow rate in VSWS is defined according to the available driving pressure differential and the pressure loss characteristics of components in the wall system.

These pressure loss characteristics are determined by the geometry of the ventilated chamber, geometry and size of vent openings, and by the surface roughness characteristics of the wall cavity. These wall system characteristics are not commonly considered in HVAC applications. For instance, the ventilated chamber typically comprises of a rectangular duct with extremely high aspect ratios, interior surfaces with irregular surface

* Corresponding author.
E-mail address: ddavidovic@sgh.com (D. Davidovic).

0360-1323/$ – see front matter © 2011 Elsevier Ltd. All rights reserved.
doi:10.1016/j.buildenv.2011.04.002

roughness and with random obstructions installed in the cavity for structural purposes. Herein, the chamber aspect ratio is defined as the chamber width-to-depth ratio and follows widely accepted terminology for design of ducts in HVAC industry. A simple comparison of the dimensions of the ventilated chamber with the standard dimensions of ducts used for air distribution in HVAC systems indicates that the current methodology for the design of duct systems defined by ASHRAE cannot be applied directly to wall systems.

The air velocities in a ventilated chamber are significantly lower than the values recommended for HVAC duct design. For example, the lowest velocities recommended for low-pressure duct systems and round ducts found in the friction chart [1] are approximately 2.0 m/s with a pressure drop of 0.7 Pa/m. The average air velocities in the ventilation chamber rarely reach even the lowest range of velocities recommended by ASHRAE for duct design. For a typical residential wall assembly consisting of brick veneer cladding, 1.22 m wide and 2.4 m high, 20 mm deep cavity with two open head joints both at the top bottom, measured in-service natural ventilation rates varied between 0 and 90 ACH [12], indicating the maximum averaged air velocity in the ventilated chamber of 0.06 m/s. Corresponding Reynolds numbers for this particular wall assembly and maximum ventilation rates would be: Re =160–180, depending on the temperature of ventilating air, clearly indicating that laminar flow regime prevails in the majority of ventilating chamber space. Pursuing the simplified procedure for estimates of local and friction pressure losses, as described in [11], the pressure drop due to friction losses at maximum ventilation rates would be order of magnitude smaller O(10^{-1} Pa) when compared to local pressure drop through the top and bottom weep vents O(10° Pa) , mainly due to small heights and low air velocities. This illustrative example shows not only very low magnitudes of friction pressure losses calculated by available simplified analytical procedures for this particular wall assembly, but also the difficulties associated with accurate measurement of air velocities and frictional pressure losses in the wall cavity under field conditions. The accurate measurement and prediction of pressures losses and the air velocities in the ventilated chamber is, therefore, of vital importance.

The main objective of this study is to identify the analytical model best suited to estimating the available airflow rate through the VSWS once the available pressure differential at the inlet and outlet vent openings is known. An exact quantification of the driving pressure differential caused by the natural driving forces is beyond the scope of this paper. Hence, the study focuses mainly on the characteristics of the airflow through the vent openings with low Reynolds numbers (laminar and transitional flow regimes) and ignores the influence of frictional pressure losses caused by the surface roughness characteristics of ventilated chamber walls.

2. Approach

It is well known from fluid mechanics theory that the total pressure loss in any fluid flow system with complex geometry cannot be represented as the simple sum of the local pressure losses through its components as long as the local losses interfere with each other. The mutual influence of local pressure losses cannot be neglected when they occur in proximity to each other, and the flow disturbance created at one location affects the flow field at another location. However, there are two practical reasons for dividing the ventilated screened wall system into subsections. The first is to create a classification of pressure losses based on the type and place of occurrence. The second is to develop a unique methodology for calculating constitutive pressure losses and overall pressure loss through the system. This approach, however, may lead to certain loss of accuracy in the estimate of the total pressure loss within the system. Depending on the flow and geometry characteristics, it is useful to divide the ventilated wall chamber into several characteristic flow zones following the airflow path through the wall assembly. This approach is illustrated in Fig. 1.

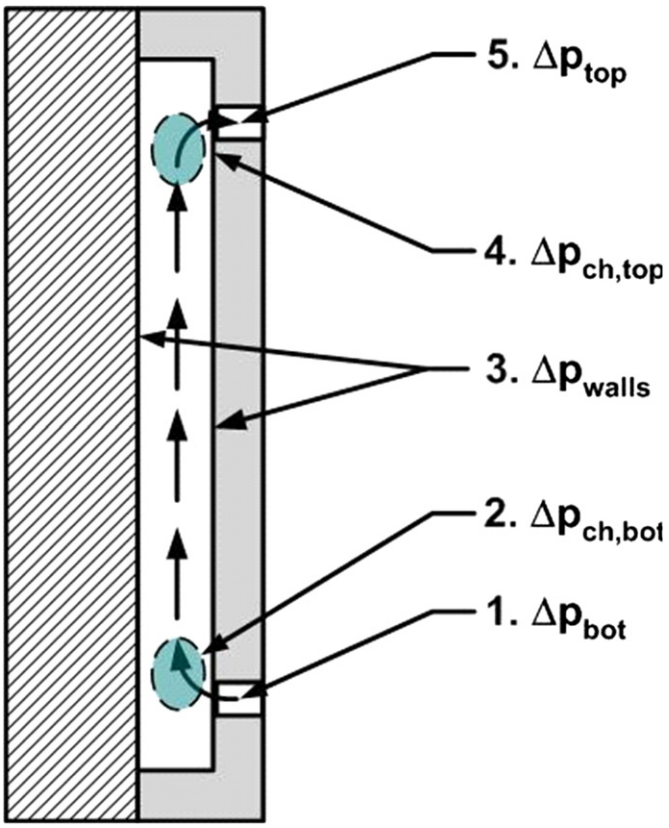

Fig. 1. Classification of pressure losses in ventilated screened wall systems (VSWS).

Assuming an upward direction of the airflow, which is the typical scenario in winter, the pressure losses in ventilated and screened wall systems (VSWS) may be assigned to distinctive flow zones as:

1. Δp_{bot} – the local pressure loss through the bottom opening (in this case, the inlet vent),
2. $\Delta p_{ch,bot}$ – the local pressure loss due to the change of stream direction at the bottom,
3. Δp_{wall} – the pressure loss due to friction in the ventilated chamber,
4. $\Delta p_{ch,top}$ – the local pressure loss caused by the change of the stream direction before the top opening, and
5. Δp_{top} – the local pressure loss through the top opening (in this case, the outlet vent).

The calculation of pressure losses for many practical applications in the design of HVAC systems assumes independent estimation of frictional and local losses of the components in the system. The standard approach for estimating frictional pressure losses in ducts uses the widely known Darcy–Weisbach equation to determine the friction factor, taking into account the flow regime through Reynolds numbers and the wall surface roughness characteristics through equivalent roughness heights.

The local pressure losses are calculated using local loss coefficients, usually provided as tabulated C, K or ζ values for various

geometric conditions and flow regimes (laminar or turbulent flow). Viscous friction at the chamber walls typically contributes little to the overall pressure loss characteristics of VSWS and pressure losses due to viscous friction in the ventilated chamber are not considered, although some applications with very rough wall surfaces may require special consideration. The intention here is to provide reliable analytical tools to quantify the local pressure losses through the inlet and outlet vents, taking into account the change in air stream direction in the vicinity of the vent openings.

Significant effort was invested in experimental work to determine the local pressure losses for numerous fitting arrangements in industrial applications. Experimental data for many different fittings and geometries used primarily in typical HVAC systems and industrial facilities are tabulated [1–4]. Unfortunately, none of the cited resources provide reliable data relevant to calculation of pressure losses in VSWS.

The influence of local pressure losses further complicates the problem, as follows: the disturbances created by the flow of ventilated air through the vent openings of various shapes may affect pressure losses due to the change of direction in the air stream immediately after these openings. In such cases the total pressure loss cannot be treated simply as a sum of local pressure losses without taking their interaction into account. However, some researchers argue that this interaction may be ignored because the air velocities in the ventilation chamber after the vent openings are so low [5]. The pressure loss caused in that manner may be negligible due to the relatively low momentum of the air stream after expansion at the vent outlets. One way of avoiding this problem is to combine these two local pressure losses into single, equivalent local pressure loss.

Most useful analytical models for this study are available in a comprehensive handbook on hydraulic resistance [3] and the ASHRAE Duct Fitting Database [2]. The majority of the tabulated values for local loss coefficients in Ref. [2] originate, however, from Idelchik's work [3]. Other literature sources such as Refs. [6–8] also provide some useful information about this topic. These analytical models be used as primary resources to estimate the potential for natural ventilation in VSWS and for quantifying the local pressure loss coefficients through both discrete and slot vent openings. In order to validate the reliability and accuracy of available analytical models for estimating local pressure losses in VSWS, it is highly recommended to conduct either laboratory or field experiments, because universally applicable analytical models still do not exist for each particular configuration of vent openings and various wall claddings. The alternative path in the validation process of analytical models for local pressure losses in VSWS wall systems may involve numerical modeling using computational fluid dynamics, as it emerged as a promising and well established engineering tool in the last few decades.

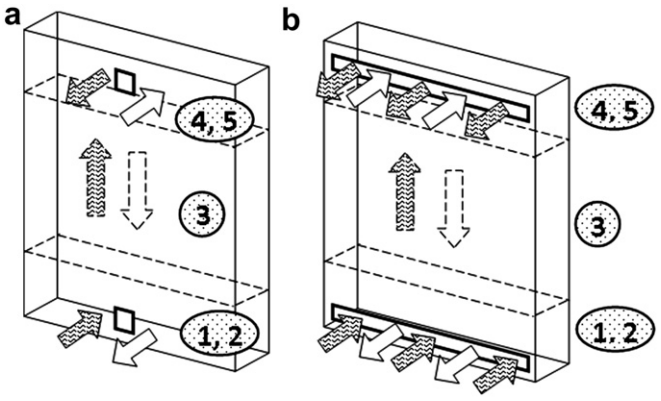

Fig. 2. Characteristic flow zones in ventilated screened wall system (VSWS) with (a) small and regular (discrete) vents and (b) slot vents.

Assuming negligible local pressure losses due to a change of stream direction after the single vent, the ventilated chamber can be divided into three characteristic regions. Three flow zones characterized by significant and measurable pressure losses are presented in Fig. 2. An attempt was made to group the pressure drops due to airflow through the orifice with pressure drops due to change of the flow stream direction close to the vent and slot openings (zones **1** + **2** and **4** + **5** in Fig. 2), and to decouple them from the purely frictional pressure drop through the rest of the wall cavity (zone **3**).

It is important to emphasize the complexity of the flow field in zones **1** + **2** and **4** + **5** with regard to ventilation strategy and vent flow geometry. The overall pressure drop is caused by the simultaneous influence of the flow through the vents and the change in stream direction after/before passage through the vents. Moreover, the flow pattern at zone **1** + **2** is considered to be different from the flow pattern at the outlet opening (zone **4** + **5**) due to the nature and sequence of the pressure drops that occur. Not surprisingly, the pressure drop in each of these zones is expected to have a different value. The nature of the flow and decoupling of the pressure losses within these zones requires further research and more detailed analysis. Experimental investigations using advanced flow visualization and flow measurement techniques combined with numerical modeling of the flow using computational fluid dynamics appear to be valuable tools in establishing better analytical correlations for local pressure drop characteristics within these zones.

It is assumed that the airflow through zone **3** is fully developed. In most cases the flow regime within this zone will be laminar (in the wall system with small discrete vent openings) or may fall into transient region (in the wall system with slot vents). The turbulent mixing of the airflow after the inlet vent openings is intense; however, it is supposed to decay relatively fast. The main concern in the flow analysis is to define accurately the beginning and the end of zone **1** + **2** along the wall height. Similarly, it is essential to establish accurate location for flow disturbances near the exit vents (zones **4** + **5**). Due to nature of the flow, the disturbed flow region at the vicinity of exit vents will most likely occupy much smaller space of the ventilated chamber volume when compared to affected region at the inlet vents. These considerations are also of great importance to the proper positioning of pressure transducer taps in experimental setups. Nevertheless, it is presumed that main contributors to the pressure drop through the system appear at the vent and slot openings (zones **1** + **2** and **4** + **5**).

Intuitively, it is generally assumed that airflow enters the ventilated chamber at the bottom and exits the space through the top opening (hatched arrows). This assumption is valid in winter, when the cold outside air enters the cavity space at the bottom, gets warmed in the cavity, and as warm air with lower density moves up and leaves the space through the top opening. However, in summer, the direction may be reversed. Warm air in the ventilated chamber is cooled once inside, becomes heavier, exits the chamber through the openings at the bottom, and gets replaced by warmer exterior air through the top openings. Flow due to stack effect can be reversed even in a day and night scenario. It is also worth noting that wind pressure can also alter the flow direction through the ventilated chamber regardless of temperature conditions.

3. Review of theoretical models

This section provides a detailed overview of existing analytical methods for estimating the ventilation flow rates and pressure drop characteristics through discrete and slotted vent openings, used primarily in the theory of natural ventilation and infiltration of the indoor spaces in buildings. The literature review revealed

four basic groups of analytical models based on the apparent flow features:

- Flow through cracks,
- Flow through gaps/slots,
- Orifice flow, and
- Entrance/exit flow models.

An attempt is made to examine in detail the characteristics of the available models and to determine the most suitable models for use in evaluating the local pressure losses through the vent openings in the VSWS.

3.1. Crack flow models

3.1.1. Crack flow approach

An expression that relates the pressure drop and volumetric flow rate through the cracks originates from the widely used power law approach and is defined as [19]

$$\Delta p_c = K \cdot Q^n, \tag{1}$$

According to [16], its applicability is limited to small openings with a characteristic dimension smaller than 10 mm where the width of the crack is typically adopted as the characteristic dimension. The coefficients K and n in Eq. (1) can be derived directly for the crack flow. Based on the crack geometry, the coefficients K and n are calculated according to following expressions available in Refs. [6] and [10]:

$$K = L_{cr} \cdot 9.7 \cdot (0.0092)^n, \tag{2a}$$

$$n = 0.5 + 0.5 \cdot \exp(-500 \cdot W_{cr}), \tag{2b}$$

where K is in [l s^{-1} Pa^{-n}], L_{cr} is crack length in [m], and W_{cr} is crack width in [m]. The model equations (2a) and (2b) were originally proposed by Ref. [11]. A similar form of Eq. (1) is available in the literature where the crack length is presented as a variable [6]:

$$Q_{cr} = k \cdot L_{cr} \cdot (\Delta p_c)^n. \tag{3}$$

The variation of the exponent n in Eq. (3) is not large, with average values around 0.6–0.7. However, the coefficient k shows a larger deviation for cracks around the windows for a value of fixed n [6].

The proposed relationship in Eq. (1) has been found to be useful for a wide range of crack geometries. The exponent value n adopts an approximate value of 1.6 [12]. However, equations formulated in this manner are not dimensionally homogeneous and are in direct conflict with a fundamental law of fluid mechanics – Reynolds law of similitude – according to the same author.

Some authors report that the flow rate is approximately proportional to the square root of the pressure drop through the crack [9], i.e.

$$Q = a \cdot \sqrt{\Delta p}, \tag{4}$$

where a is a constant proportional to the effective leakage area (ELA). Unfortunately, this approximation cannot be used universally for any type of crack geometry and any pressure differential, for various reasons. For instance, a variation in the discharge coefficient (C_D) of the opening produces a deviation from this approach. The discharge coefficient takes into account the contraction of the stream flowing through the vent opening as well as the effects of swirling flow and turbulent motion near the opening, and all these effects have strong influence on the discharge coefficient values. An expanded form of Eq. (4) using the discharge coefficient as a variable is

$$Q = C_D \cdot A \cdot \sqrt{\frac{\Delta p}{\rho}}. \tag{5}$$

Eq. (1) is a general form of the power law relationship between the volumetric flow rate Q and pressure drop Δp for a wide range of crack geometries. Some authors ([9,13]) suggest using the quadratic relationship for calculating the pressure drop through the openings in building enclosures caused by natural ventilation. The same formulation is found in Ref. [7]. The quadratic dependence of the pressure drop on the volumetric flow rate is expressed as

$$\Delta p_c = \alpha \cdot Q^2 + \beta \cdot Q. \tag{6}$$

The apparent advantage of Eq. (6) is the actual separation of the laminar and the turbulent portion of the flow. For laminar flows, the pressure drop through the opening is proportional to the flow rate (described by the second term in the right hand side of the expression above). However, for turbulent flows, this relationship approaches quadratic behavior (modeled through the first term on the right hand side of the expression above).

The crack flow approach, although extensively used in natural ventilation and infiltration of buildings, has several weaknesses. It is dimensionally non-homogeneous, and coefficients in the equation can vary significantly for different opening geometries. The quadratic approach which treats the laminar viscous losses and turbulent local losses separately is suggested as a better alternative. The experimental work conducted by Ref. [9] justified the use of the quadratic approach in a wider range of low-flow regimes and geometries compared to the power law approach.

3.1.2. Power law approach

The power law equation has been widely used to describe pressure drops through ventilation openings [13]. The equation can be written in two different ways, but the same methodology is applied to describe airflow through the openings. A two-parameter power law curve is defined as

$$\Delta p_{op} = \alpha \cdot Q_{op}^{\beta}, \tag{7}$$

or

$$Q_{op} = C \cdot \Delta p_{op}^{n}. \tag{8}$$

The term Δp_{op} represents the total pressure drop through the vent opening, while the constants α, β, C and n are assumed to be dependent only on the geometry of the vent opening. These techniques are commonly used to measure infiltration flow rates in many buildings, and it was empirically determined that the flow vs. pressure curve follows this pattern [14]. In a theory, the exponent n takes values between ($n = 1/2$) for inertial (turbulent) flow and ($n = 1$) for laminar flows. The value of the exponent depends on the relative contribution of viscous and inertial (kinetic) forces to the total pressure loss [15]. For low driving pressure differentials, the viscous forces dominate the motion of airflow and the flow rate is proportional to the applied pressure differential, as described by Hagen–Poiseuille's equation. Higher driving pressure differentials result in larger flow rates, and the flow regime approaches transitional and turbulent conditions with flow rates proportional to the square root of the applied pressure differential [16].

Unfortunately, this relationship is not universally applicable to all types of cracks, crack geometries and pressure differentials [9]. Experimental tests on many buildings show that the exponent n in Eq. (8) has a value of 2/3 with a standard deviation of SD = 0.09 [14].

This value typically varies from 0.5 to 0.7 in calculations of the air infiltration rates through the building envelope in residential applications. Many authors and researchers recommend adopting values of 0.65–0.67 as a good starting point in estimates of air infiltration rates.

The assumption that the coefficients in the power law equation are dependent on the geometry of the openings only is still the subject of debate among scientists and engineers. Some hold that these coefficients, the exponent in the equation in particular, also depend on the nature of the flow included through the Reynolds number [13]. It was found that coefficient β varies not only with the geometry of the opening but also with the change in flow rates, i.e., with the Reynolds number. The functional equation that describes this behavior is given in Ref. [13] as: $\beta = f((L/D_h)\cdot(1/Re))$.

The different forms of Eqs. (7) and (8) with slight modifications have been used in many computer programs for airflow models in multi-zone structures, and Ref. [17] provides a good overview of the multi-zone models including various approaches to model the airflow through cracks and openings.

Comparing Eq. (1) with Eqs. (7) and (8), the crack flow and power law models use a similar approach to quantify the pressure drop through the openings as a function of the flow rate. The most significant difference between these two approaches arises merely from the categorization of cracks with respect to crack dimensions. The comments regarding the crack flow approach stated above are also valid for the power law approach.

3.2. Gap/slot flow models

3.2.1. Flow through gaps

The flow through the vent openings in walls may be considered as flow through the orifice between two infinite flow domains. Pursuing the same methodology described by Eq. (6), Ref. [8] recommended the quadratic relationship to calculate the pressure drop through the air gaps:

$$\Delta p_{op} = Q\cdot(S_g + S_e) = Q\cdot(S_g + S'_e\cdot Q) = S_g\cdot Q + S'_e\cdot Q^2, \qquad (9)$$

where $S_g = (12\rho\nu L)/(b^2A)$ [Pa/((m³/s)] accounts for the resistance to airflow through the inner part of the air gap, with the assumption that laminar flow governs this region. This assumption is valid for a relatively low Reynolds numbers (lower than 2000), where the Reynolds number is defined as:$Re = (Q2b)/(\nu A)$ (see Fig. 3). The entrance and exit resistance pressure losses are taken into account by the second term S_e in Eq. (9): $S_e = (1/2)\cdot(1.8\rho/A^2)$ [Pa/(m³/s)²] with A – [m²] defined as the cross-sectional area of the gap. A schematic of the described model is presented in Fig. 3. Depending on the driving pressure magnitudes and available ventilation flow rates, the gap flow model may be applied to situations where product of the characteristic dimension and air velocity through the vent (w) satisfies the following criterion: 2 b w < 0.24 – 0.3 for typical in-service ventilating air temperatures: −20 °C to 20 °C. The proposed mathematical formulation for the flow through the gaps resembles to the quadratic dependence of the pressure losses through the cracks described by Eq. (6), except that the linear term quantifies the pressure drops through the inner part of the air gap and the quadratic term accounts for entrance and exit pressure losses in lieu of laminar and turbulent pressure loss components defined by Eq.6 for flows through the cracks.

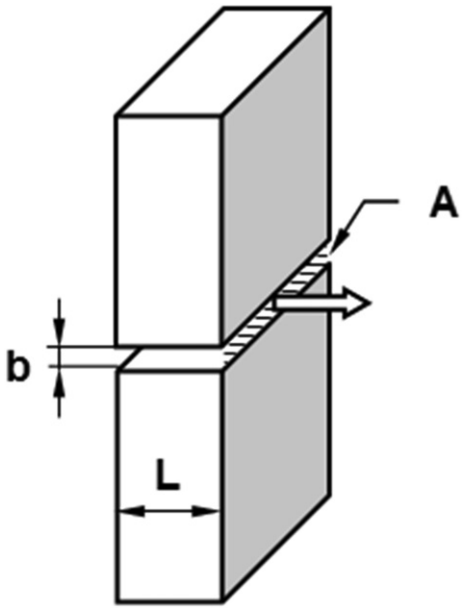

Fig. 3. Airflow through gaps approach.

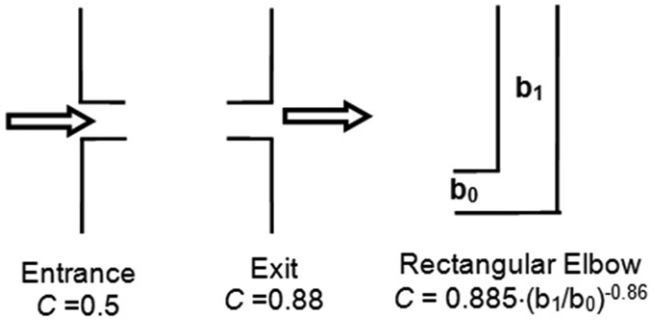

Fig. 4. Local loss coefficients for slot openings [11].

3.2.2. Slot openings

Several approaches for discrete vent openings are discussed in the preceding sections. Some of them may also be used to describe the pressure loss characteristics of slot openings. Among the others, the air gap and crack flow approach are preferred for modeling the flows and corresponding pressure losses in slot openings.

Considering typical depths of the ventilated cavities and typical slot vent dimensions, the flow through slot openings can be approximated with the flow through elbows. The following relationship is also available in [11] to estimate the local loss coefficient in sharp elbows and has been extensively used by European designers (see Fig. 4 and rectangular elbow illustration):

$$\zeta = 0.885\cdot\left(\frac{b_1}{b_0}\right)^{-0.86}. \qquad (10)$$

The equation for a sharp rectangular elbow is adopted from European literature [18] and [19]. However, its accuracy and applicability in various flow regimes (laminar, transitional or turbulent) has not been proved yet.

In general, the flows through the elbows are characterized by the eddy zone forming on the inner wall immediately after the elbow turn, due to momentum of the turning stream and its inability to adapt to new flow conditions instantly. The eddy zone formed near the corner edge contracts the flow stream after the turn, and the velocity reaches the maximum at certain distance from the elbow (similar to the vena-contracta effect). The stream starts to expand again until the flow spreads over the whole cross-section of the elbow branch.

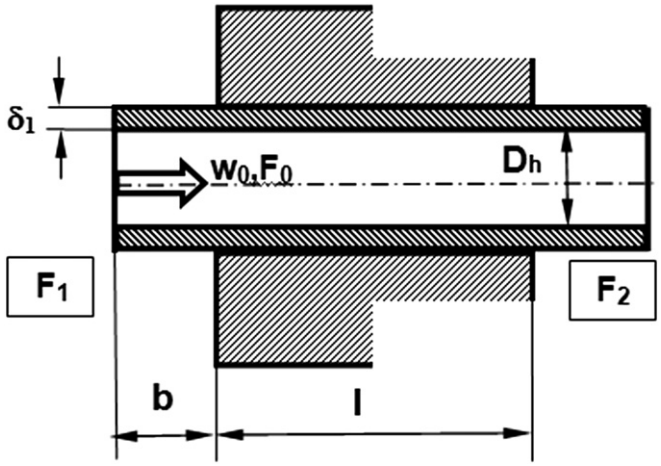

Fig. 5. Entrance into straight tube of constant cross-section, $Re < 10^4$.

According to Ref. [3], the flow resistance of elbows with flows discharging into a large volume, depends on the length of the discharge section after the elbow turn. Initially, the pressure loss increases with an increase in discharge length approximately up to characteristic width of the rectangular elbow (b_0). At this location the formed eddy zone has the largest width and creates the largest velocity across the cross-section of the duct due to vena-contracta effect. At larger discharge lengths, the pressure loss decreases and establishes a constant value regardless of the discharge length. With no discharge section after the elbow turn, the eddy zone and separation of the stream disappears, resulting in exit of the stream into the larger volume at a lower velocity, and is characterized with lower values for the local loss coefficient. However, the decrease in the local resistance coefficient is not quite substantial when compared to maximum local pressure losses observed at the location with maximum width of the formed eddy zone after the elbow turn. The minor decrease in local pressure losses is caused by the action of inertial forces which produce a compression of the fluid at the opposite wall of the elbow, thus still resulting in higher velocities at the exit section when compared to the averaged cross-section velocity at the exit. However, the described flow features are more relevant to flows with high velocities and larger stream momentum, and are more applicable to fully turbulent flow regimes. The flow of air through the VSWS with slot vents occurs with relatively low velocities for most of the time and is characterized either by laminar or transitional flow regimes, along with intermittent occurrences of low turbulence intensity flow regimes.

The flow pattern described above may not be completely adequate to portray the flow features at the exit vent openings in VSWS. For such flows, Ref. [3] recommends using the expression for pressure loss coefficients derived for any-edge orifice in laminar and transitional flows. This analytical model is reviewed in detail in subsequent sections of this paper.

The obvious advantage of the proposed models for local pressure loss estimates in slot openings is the independence of the local loss coefficients from the Reynolds number and its variability solely on the slot opening and ventilated chamber geometry.

3.2.3. Entrance into straight tube

The following formula is proposed by Ref. [3] to describe the pressure loss of flow through the entrance opening in a wall with a expansion downstream at the tube exit ($F_1 = \infty$, see Fig. 5):

$$\zeta = \left[\zeta' + \left(1 - \frac{F_0}{F_2}\right)^2 + \tau \cdot \left(1 - \frac{F_0}{F_2}\right) + \zeta_{fr}\right], \tag{11}$$

where ζ' is the coefficient depending on the shape of the orifice inlet edge, and $\zeta_{fr} = f \cdot (l/D_h)$ represent the contribution due to friction in the entrance tube to overall local loss coefficient. For vent openings in very thin claddings such as metal panels, fiber cement clapboards or vinyl siding claddings, t, this term may be neglected. However, brick veneer wall systems are typical examples of wall systems where this coefficient may contribute significantly to the overall pressure loss through the vent.

Fig. 5 depicts the vent opening geometry characteristics relevant for local pressure loss estimates. The coefficient ζ' takes into account the shape of the inlet and depends on both the thickness of the inlet tube (δ_1) and the misalignment of the inlet tube with the wall face (b). Ref. [3] provides tabulated data and detailed diagrams with the resistance factor curves plotted as a function of these two variables. Unfortunately, the complexity of reported analytical expressions and the complexity of the provided curves limit the use of this model for practical applications.

In order to reduce the complexity of the proposed model and to make it easy-to-use in building science applications, the coefficient ζ' may be approximated by the value for the resistant coefficient at the entrance into a straight tube of infinitely small thickness. In that way, the resistance coefficient value ζ' varies between 0.5 and 1.0 as given in Table 1, and allows some mathematical manipulations such as curve fitting to enhance its practicability. Following the proposed methodology, dimension b represents the thickness of the vent opening projecting out from the cladding wall which may replicate the situations where plastic tube are inserted in the weep hole openings in the cladding wall systems with brick veneer. The coefficient τ accounts for the effect of the thickness of the opening wall and the inlet edge shape, and it may be assumed to have a constant value for thick-edge orifices:

$$\tau = (2.4 - \bar{l}) \times 10^{-\varphi(\bar{l})}, \tag{12}$$

$$\varphi(\bar{l}) = 0.25 + 0.535 \cdot \bar{l}^8 / \left(0.05 + \bar{l}^7\right) = 0.25, \tag{13}$$

assuming $\bar{l} = l/D_h = 0$, where l is the thickness of the vent opening in the wall, and D_h is the hydraulic diameter of the vent opening. The coefficient τ tends to a constant value of 1.35 for an infinitely thin-edge orifice, and approaches zero value for very thick orifices.

This approach may also be applied to estimate the local pressure losses through the slot openings by adopting the hydraulic

Table 1
Entrance into a straight tube [3].

Resistance coefficient: ζ'											
δ_1/D_h	b/D_h										
	0	0.002	0.005	0.010	0.020	0.050	0.100	0.200	0.300	0.500	∞
0	0.50	0.57	0.63	0.68	0.73	0.80	0.86	0.92	0.97	1.00	1.00

diameter (D_h) to be equal to double height of the slot opening, i.e.: $D_h = 2h$.

For the outlet vent opening, Ref. [3] recommends the similar model:

$$\zeta = \left[1 + \zeta' \cdot \left(1 - \frac{F_0}{F_1}\right)^{3/4} + \tau \cdot \sqrt{\left(1 - \frac{F_0}{F_1}\right)^{3/4}} + \zeta_{fr}\right] \cdot \left(\frac{F_1}{F_0}\right)^2. \quad (14)$$

This approach has been used quite often to model the pressure losses by discharging the fluid from the vent opening into an infinite space at the end of the tube ($F_2 = \infty$). The other terms in Eq. (14) have the same function as the parameters described in Eq. (11), and the expressions described above by Eqs. (12) and (13) are equally applicable to the outlet vent openings.

Simplifications of this model are introduced through dependency of the coefficient ζ' only on the thickness of the vent opening projecting out from the cladding wall (b), as it was adopted in the inlet vent opening model. The only exception in the model is that recommended value for exit vent openings in thick walls should approach: $\zeta' = 1$ (typical Borda–Carnot exit loss coefficient). Similarly the constant value of 0.88 (as shown in Fig. 4) can also be used for calculations of local pressure losses through the outlet slot openings.

Both proposed models (entrance into the straight tube and discharge from the straight tube) are derived for uniform velocity profiles at the inlet/outlet openings and do not consider any velocity variations, incident angles, or turbulence effects in the approaching or discharging stream. The author restricted the applicability of the described models to fully turbulent flows through the vent openings with Reynolds numbers:$Re = (w_0 \cdot D_h)/\nu \geq 10^4$.

3.3. Orifice flow models

Flow through orifices has undergone extensive scientific study, and has been a subject of interest in many engineering disciplines. The process industry is the engineering field which uses orifices most extensively and for various purposes, primarily as flow measurement devices in industrial facilities. However, the literature review did not reveal a comprehensive record of using the orifice models and their variations to quantify the airflow rates in VSWS. This section aims to systematically summarize available models to quantify the pressure losses through discrete vent openings, starting from the simplest sharp-edge orifice flow and introducing more advanced analytical concepts such as any-edge orifice in laminar and transitional flows, entrance/exit flows, and sudden contraction/expansion flows.

3.3.1. Sharp-edge orifice approach

For openings with various edges located in a wall with an infinite surface area (passage through an opening from one large volume to another), the local resistance coefficient is defined as [3]

$$\zeta = \frac{\Delta p_{op}}{\rho \cdot w_0^2/2} = \zeta' + \tau + 1 + \zeta_{fr}. \quad (15)$$

Coefficient ζ' depends on the shape of the opening inlet edge; τ is the coefficient that represents the effect of the thickness of the wall, the inlet edge shape of the opening, and properties of the flow passage through the vent opening. The coefficient $\zeta_{fr} = f \cdot (l/D_h)$ represents the friction losses over the entire depth of the vent opening, where f is the friction factor of the walls in the vent opening.

It is straightforward to derive the relationship between the discharge coefficient (C_D) introduced in Eq. (5) and local resistance coefficient (ζ) in the following manner:

$$C_D = \frac{1}{\sqrt{\zeta}}. \quad (16)$$

According to Ref. [3], for thin, sharp-edged orifices $\zeta' = 0.5$, $\tau = 1.41$ and $\zeta_{fr} = 0$. These assumptions result in total value of the local resistance coefficient $\zeta = 2.91$ ($C_D = 0.586$). This value is, however, valid only for Reynolds numbers (Re) greater than 10^5 which implies the fully turbulent flow regime through the sharp-edge orifice. The same author proposed the local resistance coefficient values to vary in the range: $\zeta = 2.7–2.8$, which results in the following values for the discharge coefficient: $C_D = 0.598–0.608$. The reported values are valid under following limitations: $l/D_h = 0–0.015$ and $Re = (w_0 \cdot D_h)/\nu \geq 10^4$ and have been experimentally confirmed [3].

Kirchhoff was the first to perform the theoretical analysis needed to derive the analytical solution for the contraction coefficient (C_C) of the jet of liquid emerging through a circular orifice [20]. The analytical expression derived for the contraction coefficient of the inviscid fluid flowing through the circular hole in thin plane wall is very simple: $C_C = \pi/(\pi + 2) = 0.611$. The corresponding value of the local resistance coefficient for a circular orifice with above mentioned assumptions is: $\zeta = 2.679$. These values have been widely deployed in building science as an engineering rule of thumb to estimate the pressure loss characteristics of the discrete openings in the building envelope. The coefficient is derived for a two-dimensional jet emerging from the orifice using the free streamline theory and irrotational flow of the inviscid fluid [20]. Tabulated values for contraction coefficients derived for liquid jets discharging at different angles at the end of the pipe for different orifice opening and wall surface area ratios using two-dimensional theory are available in [21]. According to two-dimensional theory, for infinitely small orifice opening in the large plane wall, the difference between the contraction coefficient and the discharge coefficient becomes negligible.

The sharp-edge orifice approach requires a fully developed turbulent flow to be applicable. Nevertheless, in the vast majority of situations encountered under field conditions, the Reynolds numbers for the vent openings in VSWS do not fall within this range. Therefore, using the sharp-edged orifice approach to quantify pressure losses through vent openings is unlikely to produce accurate results and may not result in the actual flow rates through the vent openings. For that reason, laminar and transitional flow through the orifice with any edges [3] appears to be a viable alternative to the sharp-edge orifice model.

3.3.2. Any-edge orifice approach in laminar and transitional flow

In order to quantify the pressure losses through the orifice in laminar and transitional flows separately, [3] presents independent expressions for the local resistance coefficient using Reynolds number ($Re = (w_0 \cdot D_h)/\nu$) as the qualitative criterion to distinguish these two flow regimes:

At $30 < Re < 10^4 \div 10^5$:

$$\zeta = \left(\frac{1}{\varphi^2} - 1\right) + \frac{0.342}{\varepsilon_0^2 \cdot Re} \cdot \left[1 + 0.707\sqrt{\left(1 - \frac{F_0}{F_1}\right)^{3/4}} - \frac{F_0}{F_2}\right]^2 = \zeta_\varphi + \overline{\varepsilon}_{0Re} \cdot \zeta_{0quad}; \quad (17a)$$

where the upper limit for the Reynolds number is $Re = 10^5$ for sharp-edged orifices (restricted to cases with: $l/D_h \leq 0.015$) and

approximately $Re = 10^4$ for orifice with other edge shapes. The coefficient φ represents the velocity coefficient of discharge from the sharp-edged orifice, which is a function of the Reynolds number, and the ratio of the vent opening area and the inlet manifold area F_0/F_1(see Fig. 5).

$$\text{At } 10 < Re < 30: \ \zeta = \frac{33}{Re} + \bar{\varepsilon}_{0Re} \cdot \zeta_{0quad}; \tag{17b}$$

$$\text{At } Re < 10: \ \zeta = \frac{33}{Re}. \tag{17c}$$

The pressure drop through the orifice opening is defined as:$\Delta p = \zeta \cdot \rho \cdot (w_0^2/2)$ and the Reynolds number is calculated for the opening cross-section area: $Re = (w_0 \cdot D_h)/\nu$. The coefficient $\bar{\varepsilon}_{0Re}$ in Eqs. (17a) and (17b) contain the term representing the fluid jet area ratio ($\varepsilon_{0Re} = F_{con}/F_0$) of the sharp-edged orifice section at $F_0/F_1 = 0$ (with $F_1 = \infty$), which is defined as [3]

$$\bar{\varepsilon}_{0Re} = \frac{0.342}{\varepsilon_0^2 \cdot Re} = \sum a_i \cdot [\lg(Re)]^i. \tag{18}$$

The coefficients in Eq. (18) have the following values: $a_0 = 0.461465$; $a_1 = -0.2648592$; $a_2 = 0.2030479$; $a_3 = -0.06602521$; $a_4 = 0.013\,25519$; $a_5 = -0.001058041$. The introduced coefficient $\bar{\varepsilon}_{0Re}$ accounts for additional pressure losses due to the contraction of the stream flowing through the orifice in laminar and transitional flow regime. Separation of the flow downstream of the orifice inlet edges results in the formation of eddy zones which dissipate the energy from the main stream. If the vent opening had sufficient thickness (thick-edge orifice) it would be possible for the air stream to reattach to the vent opening walls. However, detailed experimental or numerical examination is required to estimate the reattachment point accurately and to make a clear distinction between the separated zones and fully developed flow through the vent openings. To stay on the conservative side it is recommended that the frictional losses through the vent opening be taken into account along the entire length regardless of the occurrence of separation zones.

As described above by Eq. (17a), the expression for the discharge resistance coefficient $\zeta_\varphi = (1/\varphi^2 - 1)$ is a function of the Reynolds number and ratio of the cross-sectional areas of the vent opening and inlet manifold. The plotted values and tabulated data for the discharge resistance coefficient available in [14] match each other; however, the cited empirical equation of relatively complex form does not provide a good fit to plotted and tabulated values, most likely due to some typing error. In order to avoid any misinterpretation and possible typing errors in the cited equation, the tabulated values are fitted with the polynomial equation using logarithmic function of Reynolds number (*Re*) as an argument and for the ratios of cross-sectional areas equal to or approaching zero ((i.e., $F_0/F_1 \to 0$). The adopted assumption holds well for sparsely distributed single-vent openings in the cladding walls. Since the diagram curves are plotted in a logarithmic scale, a similar approach to Eq.18 is used to fit the plotted curve:

$$\zeta_\varphi = \sum b_i \cdot [\lg(Re)]^i, \tag{19}$$

with fitting coefficients: $b_0 = 70.01263$; $b_1 = -143.79046$; $b_2 = 126.09769$; $b_3 = -60.16205$; $b_4 = 16.79359$; $b_5 = -2.74186$; $b_6 = 0.24266$ and $b_7 = -0.00899$. The correlation coefficient: $R^2 = 0.99708$ and standard deviation of: $SD = 0.04682$ are obtained by fitting the available curve in accordance with the proposed formulae in Eq. (19).

The coefficient ζ_{0quad} describes the local resistance coefficient for the orifice in the so-called quadratic region (fully turbulent flow regime). It is determined on a case-by-case basis for different vent opening inlets (sharp, beveled, or rounded inlet edges). The expression in square parentheses on the left-hand side of Eq. (17a) is used to calculate this component of total pressure loss and indicates a lack of the influence of the Reynolds number and dependence merely on the vent geometry.

The complexity of the proposed model for the local resistance coefficient in laminar and transitional flow regimes through the orifice is evident. The complexity of the model is associated with the level of detailing in the description of the flow characteristics and contributing causes to overall energy and pressure losses. However, the higher price paid in increased complexity should be offset by the improvement in the accuracy of estimates of the local pressure losses through discrete vent openings in laminar and transitional flows in the VSWS.

3.4. Entrance/exit flow models

3.4.1. Entrance and exit approach

The local resistance of the airflow through the vent openings may be considered at first glance as the Borda–Carnot entrance and exit losses. For both cases, the loss coefficients for Reynolds numbers $Re > 10^4$ are defined as [3]

$$\zeta_{loc} = \frac{\Delta p}{\rho \cdot w_0^2/2} = \left(1 - \frac{F_0}{F_2}\right)^2 \approx 1 - \text{an abrupt enlargement}, \tag{20}$$

$$\zeta_{loc} = \frac{\Delta p}{\rho \cdot w_0^2/2} = 0.5\left(1 - \frac{F_0}{F_1}\right) \approx 0.5 - \text{an abrupt contraction}. \tag{21}$$

A more exact expression proposed by the same author for abrupt contractions based on experimental results is given as

$$\zeta_{loc} = \frac{\Delta p}{\rho \cdot w_0^2/2} = \zeta'\left(1 - \frac{F_0}{F_1}\right)^{0.75}, \tag{22}$$

where ζ' represents the coefficient which is dependent on the shape of the inlet edge of the opening (sharp- or thick-edge orifice).

3.4.2. Sudden expansion/contraction approach

For a sudden expansion of a flow with an assumed uniform velocity distribution at the outlet of the opening, Ref. [3] proposed the following relationships to evaluate the local resistance coefficient:

$$\text{At } Re > 3 \cdot 10^3: \ \zeta = \frac{\Delta p}{\rho \cdot w_0^2/2} = \left(1 - \frac{F_0}{F_2}\right)^2, \tag{23a}$$

$$\text{At } 500 = Re < 3 \cdot 10^3:$$

$$\zeta = -8.44556 - 26.163 \cdot \left(1 - \frac{F_0}{F_2}\right)^2 - 5.38086 \cdot \left(1 - \frac{F_0}{F_2}\right)^4 + \lg Re \cdot \left[6.007 + 18.5372 \cdot \left(1 - \frac{F_0}{F_2}\right)^2 + 3.9978 \cdot \left(1 - \frac{F_0}{F_2}\right)^4\right] + (\lg Re)^2 \cdot \left[-1.02318 - 3.0916 \cdot \left(1 - \frac{F_0}{F_2}\right)^2 - 0.680943 \cdot \left(1 - \frac{F_0}{F_2}\right)^4\right], \tag{23b}$$

$$\text{At } 10 = Re < 500:$$

$$\zeta = 3.62536 + 10.744 \cdot \left(1 - \frac{F_0}{F_2}\right)^2 - 4.41041 \cdot \left(1 - \frac{F_0}{F_2}\right)^4 + \frac{1}{\lg Re} \cdot \left[-18.13 - 56.77855 \cdot \right.$$

$$\left(1-\frac{F_0}{F_2}\right)^2+33.40344\cdot\left(1-\frac{F_0}{F_2}\right)^4\Bigg]+\frac{1}{(\lg Re)^2}\cdot$$
$$\left[30.8558+99.9542\cdot\left(1-\frac{F_0}{F_2}\right)^2-62.78\cdot\left(1-\frac{F_0}{F_2}\right)^4\right]$$
$$+\frac{1}{(\lg Re)^3}\cdot\left[-13.217-53.9555\cdot\left(1-\frac{F_0}{F_2}\right)^2+\right.$$
$$\left.33.8053\cdot\left(1-\frac{F_0}{F_2}\right)^4\right], \quad (23c)$$

$$\text{At } Re<10:\ \zeta\approx\frac{30}{Re}. \quad (23d)$$

The notation used in the equations above also corresponds to the dimensions defined in Fig. 5. The proposed set of equations (Eqs. (23a)–(23d)) cover the whole range of the flows that may occur in the discrete and slot vent openings in the VSWS. The sudden contraction in the transition and laminar flow regimes model can also be used to estimate the pressure losses through the discrete vent openings. According to Ref. [3], the local resistance coefficient of the flow passing through sudden contraction is defined as follows:

$$\zeta_{cont}=A\cdot B\cdot\left(1-\frac{F_0}{F_1}\right), \quad (24)$$

where coefficient: $A=\sum_{i=0}^{7}a_i\cdot[\lg(Re)]^i$ and corresponding coefficients in the sum have the following values: $a_0=-25.12458$; $a_1=118.5076$; $a_2=-17.04147$; $a_3=118.1949$; $a_4=-44.42141$; $a_5=9.09524$; $a_6=-0.9244027$ and $a_7=0.03408265$.

The complex formulation for term A in Eq. (24) may cause additional difficulties in the practical application of the proposed model requiring iterative numerical procedures to solve the problem. Further complication arises with the proposed equation for coefficient B in the form of a double series:

$$B=\sum_{i=0}^{2}\left\{\left[\sum_{j=0}^{2}a_{ij}(F_0/F_1)^j\right]\cdot(\lg Re)^i\right\}. \quad (25)$$

Table 2 provides the values for coefficients a_{ij} used in Eq. (25). Nonetheless, the local resistance coefficient values calculated by Eq. (24) and Eq. (25) are inconsistent with the values reported in the table within the same literature source [14]. Fig. 6 provides an overview of local resistance coefficient values for various flow and geometry plotted from listed values in the Table 2.

Again, the local resistance coefficient values calculated by Eqs. (24) and (25) are inconsistent with the values found in the table within the same literature source [3]. In order to make a better prediction for the local resistance coefficient of discrete vents, we extrapolated the tabulated values to cover the very small range of the area ratios (F_0/F_1) that are of most interest for proper modeling of the flow in VSWS. We divided the available data set into three distinct intervals of Reynolds number which permitted a more accurate fitting process and avoided potential difficulties for good fit in the vicinity of saddle point in higher range or Reynolds numbers, as observed in Fig. 6.

Table 2
Coefficients values for sudden contraction in laminar and transitional flow regime [14].

a_{ij} Values	$10\le Re\le 2\times10^3$			$2\times10^3\le Re\le 4\times10^3$		
i/j	0	1	2	0	1	2
0	1.07	1.22	2.9333	0.5443	−17.298	−40.715
1	0.05	−0.51668	0.8333	−0.6518	8.7616	22.782
2	0	0	0	0.05239	−1.1093	−3.1509

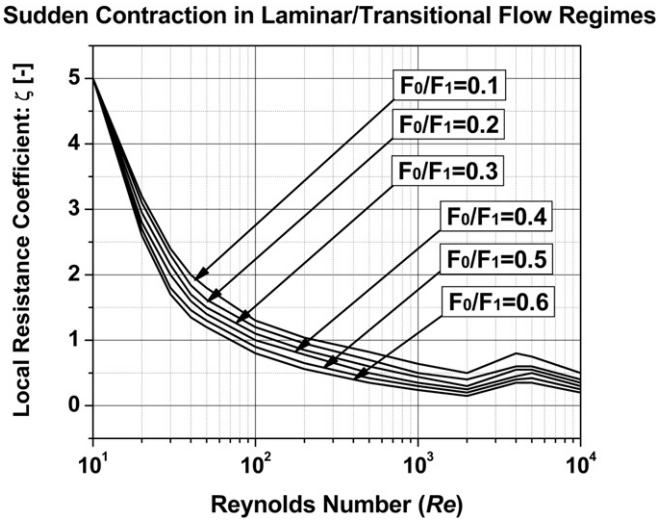

Fig. 6. Local resistance coefficients values for sudden contraction in laminar/transitional flow regimes ($Re>10^4$), adapted from Ref. [14].

The obtained values for the local resistance coefficient are fitted using the fifth order polynomial for Reynolds number lower than 2000 ($Re<2000$) in a fashion similar to that used to calculate the coefficient A:

$$\zeta=\sum_{i=0}^{5}b_i\cdot[\lg(Re)]^i, \quad (26a)$$

where the coefficients are: $b_0=25.02183$; $b_1=-39.18051$; $b_2=27.8403$; $b_3=-10.63412$; $b_4=2.13396$ and $b_5=-0.17675$. The correlation coefficient was $R^2=0.99794$, and standard deviation was $SD=0.09145$, indicating good agreement as shown in Fig. 7. The selected range of Reynolds numbers corresponds to laminar flow regimes through the discrete vents.

Simple linear correlation was used to estimate the local resistance coefficient for the range of Reynolds numbers $2000<Re<4000$, which approximates the low-end transitional flow regimes:

$$\zeta=0.0002\cdot Re+0.25. \quad (26b)$$

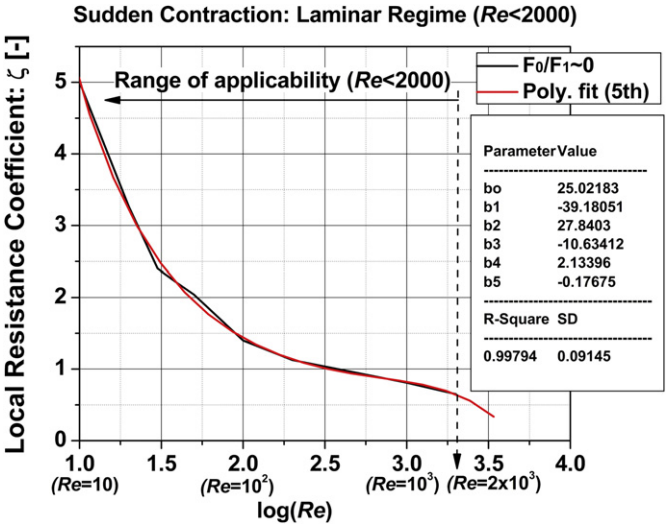

Fig. 7. Fitted values of local resistance coefficient for sudden contraction in laminar flow regime ($Re<2000$).

Table 3
Discharge from a tube made flush with the wall [14].

ζ: b/a = 5 ÷ 10					
δ (°)	W_∞/w_0				
	0	0.5	1.0	1.5	2.0
45	1.00	0.92	0.93	1.10	1.30
60	1.00	0.87	0.87	1.03	1.25
90	1.00	0.82	0.80	0.97	1.20
120	1.00	0.80	0.76	0.90	0.98

The second-order polynomial was used to model the values for the local resistance coefficient in the upper range of transitional flow regimes with Reynolds numbers ranging from 4000 to 10,000:

$$\zeta = 4.111\cdot10^{-09}\cdot\mathrm{Re}^2 - 1.270\cdot10^{-04}\cdot\mathrm{Re} + 1.49222. \quad (26c)$$

The equations, developed for the local resistance coefficient of the flows with sudden contraction at extremely low area ratios ($F_0/F_1 \to 0$) still exhibit the level of complexity present in the proposed model for the flows with sudden expansion. The overall complexity of these two models is comparable with the any-edge orifice approach in laminar and transitional flow regimes. However, the equations presented cover the whole range of Reynolds numbers most likely to occur in the discrete and slot vent openings in the VSWS (Figs. 6 and 7).

3.4.3. Discharge from tube approach

Given the similarity in the general flow characteristics, a model that describes the local pressure losses in the stream exiting the tubes and channels [3] may also be used to obtain a more accurate estimate of the local pressure through the discrete outlet vent openings. In general, the pressure loss in this scenario consists of the internal pressure loss (Δp_{int}) and the dynamic pressure loss of the jet stream at the outlet (Δp_{vel}). Depending on the position of the pressure tap at the exit of the vent opening, the dynamic pressure loss of the airflow stream may be ignored. This assumption is valid only if the pressure tap is placed relatively close to the vent opening exit to avoid the velocity decay in the air stream further away from the vent opening.

For uniform velocity profiles at the exit of the vent opening, regardless of the nature of the flow at the exit section (i.e., whether the flow is turbulent or not), the common engineering practice is to adopt the local resistance coefficient equal to one [3]. Any non-uniformity in the velocity profile increases the local resistance coefficient values. As a result of the natural movement of the outside air under windy conditions, it is possible to encounter smaller total pressure lo than commonly assumed pressure loss in the velocity pressure (i.e., at $\zeta < 1$) for certain velocity ratios of the flow stream through the vent opening (w_0) and organized bulk motion of the outside air (w_∞): $w_\infty/w_0 > 0$. For lower velocity ratios, the decrease in the local resistance coefficient is created by the "blowing effect" of the bulk air stream outside the ventilated chamber. Namely, the blowing effect produces an increase in static pressure differences across the vent opening between the air in the ventilated chamber and outside air, similar to the well-known shower curtain effect, without significant distortion of the exiting air stream through the vent opening. An increase in static pressure differential across the vent opening is equivalent to a decrease in the flow resistance coefficient since it enhances the escape of the ventilating air through the vent opening. On the other hand, further increase in the velocity of the passing stream of outside air may result in excessive contraction of the exiting air stream through the vent opening. A distinctive contraction of the air stream at the vent opening exit produces an increase in the velocity pressure of the exiting air stream and pressure loss through the vent opening increases accordingly. Obviously, the larger contraction of the stream exiting the vent opening cancels out the benefit gained by the blowing effect of the bulk air stream outside, as observed in the presented tabulated data in Table 3 below.

Table 4
Overview of available analytical models for evaluation of local pressure losses in VSWS.

Flow type	Model name	Publication source	Flow regime/geometry applicability	Complexity
Crack flow	Crack flow approach	Clarke [11] Allard [6]	- Non-homogeneous; - Violate Reynolds law of similitude; - Dimensions ≤ 10 mm.	- Simple; - Easy-to-use.
	Power law approach	Etheridge and Sandberg [13]	- Covers all Reynolds numbers; - Covers wide range of geometries; - Coefficients vary with Re and geometry (usually not taken into account).	- Simple.
Slot/gap flow	Flow through gaps (quadratic approach)	Hagentoft [8]	- Re ≤ 2000 (laminar flow); - Range of geometries limited by velocity magnitudes and Re number restriction.	- Simple.
	Slot openings	Straube and Burnet [5]	- Reynolds numbers: N/A; - Covers wide range of geometries.	- Simple.
	Entrance into straight tube approach	Idelchik [3]	- $Re \geq 10^4$ (turbulent flow); - Covers wide range of geometries.	- Medium/complex.
Orifice flow	Sharp-edge orifice	Idelchik [3]	- $Re \geq 10^4$ (turbulent flow); - Covers wide range of geometries.	- Simple.
	Any-edge orifice	Idelchik [3]	- $10 \leq Re \leq 10^{4\div5}$ (lam. & trans. flow); - Covers wide range of geometries.	- Complex.
Entrance/exit flow	Entrance/exit approach	Idelchik [3]	- $Re \geq 10^4$ (turbulent flow); - Covers wide range of geometries.	- Simple.
	Sudden contraction/expansion approach	Idelchik [3]	- $10 \leq Re \leq 10^4$ (lam. & trans. flow); - Covers wide range of geometries.	- Complex.
	Discharge from a tube	Idelchik [3]	- $Re \geq 10^4$ (turbulent flow); - Opening dimensions aspect ratios: 5–10 (single-vent openings); - Stream incident angle considered; - Presence of a passing stream modeled.	- Simple/medium.

The presence of organized air movement in the ventilated chamber may also prevent the ventilating air from approaching the vent opening uniformly from all sides. A departure from flow uniformity may also result in increased pressure and energy losses. Considering relatively low velocity ranges and corresponding low momentum of the air stream in the ventilated chamber, this effect often may be neglected from the estimates of the pressure losses for outlet vent opening. However, variability in incoming flow direction and magnitude at the inlet vent openings may require this pressure loss to be analyzed with more detail.

Data for the local resistance through a discharge from a tube flush with the wall in the presence of a passing stream are also available in Ref. [3]. Tabulated data are provided for a rectangular cross-section tube made flush with the wall in the presence of a passing stream for different angles of incidence and aspect ratios of the vent opening dimensions within the range b/a = 5–10. The range of velocity ratios and geometry shapes applies to actual situations such as discrete weep hole vents in the brick veneer cladding wall systems. Table 3 presents the local resistance coefficient values for different incidence angles (δ) and Reynolds numbers ($Re = (w_0 \cdot D_h)/\nu > 10^4$):

A second-order polynomial is used at first to fit the data through the tabulated data points for incidence angle of 90° as the most representative example of the flows through the vent opening encountered in practice. The values for 90° incidence angles are taken from Table 3 and are in good agreement with plotted curves in Ref. [3]. The fitted equation produced less than 3% of inherent error:

$$\zeta = 0.2935 \cdot \left(\frac{w_\infty}{w_0}\right)^2 - 0.4663 \cdot \left(\frac{w_\infty}{w_0}\right) + 0.9839. \quad (27)$$

In a similar manner, a third order polynomial approximation gives a slightly better correlation with an inherent error smaller than 2.5%:

$$\zeta = -0.0614 \cdot \left(\frac{w_\infty}{w_0}\right)^3 + 0.4777 \cdot \left(\frac{w_\infty}{w_0}\right)^2 - 0.6053 \cdot \left(\frac{w_\infty}{w_0}\right) + 1. \quad (28)$$

Because of its relatively simple form and smaller inherent error, the latter expression appears more appropriate for modeling the pressure drop through the outlet discrete vent openings.

4. Discussion

Table 4 presents a detailed overview and comparison of the analytical models available in the literature for calculating the local pressure losses in the VSWS. The simplest model is the crack flow model. Although it has a very simple form, it has several obvious weaknesses that affect its application. It is dimensionally non-homogeneous, and the coefficients in the equation can vary significantly for different opening geometries. Therefore, it cannot be generally applied to different ventilation strategies in the VSWS using discrete and continuous vent openings.

The power law approach has also been extensively used in calculations of the air infiltration rates through building envelopes. Needless to say, the essential characteristic of this approach is the flexibility of the coefficients and exponents in the equations to accommodate various vent opening geometries and flow conditions, which is frequently neglected in engineering practice. The quadratic approach, which treats the laminar viscous losses and local losses separately, is suggested as another option to improve the predictability of the power law model. For that purpose, the quadratic model for airflow through gaps may be used to calculate both the local pressure losses through the discrete and continuous vent openings. However, its use is restricted to flows through the gaps with Reynolds numbers lower than 2000 (laminar flow regimes). Imposed limitation on the Reynolds number may affect the applicability of gap model in various situations, i.e., the larger driving pressures for natural ventilation will result in larger ventilation flow rates and corresponding air velocities through the vent restricting the applicability of the model to smaller vent sizes and vice versa.

In order to take into account the transitional flows as relatively frequent types of flows in discrete vent openings, Idelchik's model for any-edge orifices in laminar and transitional flow is recommended as the most appropriate. Although the proposed model considers the variation of the local pressure loss coefficient with the Reynolds number, it is more complex compared to the other models, and may require implementation of iterative procedures in the calculation process. An increase in the complexity of the model and in the characterization of the local resistance coefficients should, however, result in better prediction of the pressure losses in the VSWS.

The models for sudden exit and sudden entrance are also promising options for quantifying the local pressure losses through the inlet and outlet vent openings. These models clearly possess a certain degree of complexity when compared to the well-known power law and sharp-edge orifice approach. The level of complexity of the sudden exit/entrance model approaches the one observed for Idelchik's model for any-edge orifice in laminar and transitional flows.

A model for discharge from a tube flush with the wall and in the presence of a passing stream is also proposed in the literature for use in calculating the pressure losses both through discrete and slot vent openings. The model is slightly simplified when compared to the sudden exit/entrance approach and any-edge orifice in laminar and transitional model, and it accounts only for variation in local pressure loss coefficients caused by the local geometry both of the ventilated chamber and the vent opening. Although it takes into account the presence of the air stream passing the vent opening and the incident angle of the discharging stream, it does not consider the influence of various Reynolds numbers and different flow regimes on the local resistance coefficient. Overall, we expect better performance of this model in estimates of the local pressure losses through the outlet vents regardless of the type of the vent (discrete or continuous).

5. Conclusions

The building science theory currently lacks a general methodology for the classification, measurement and quantification of local pressure losses in VSWS. An attempt has been made to transfer our knowledge of fluid mechanics, energy and pressure losses from industrial applications to a quite unique field of building science or to be more specific, to the field of natural ventilation flows of air in ventilated and screened wall systems (VSWS). The preceding sections focused on the analytical models available in the literature that are most appropriate for estimating the local pressure losses through discrete and continuous vent openings in the VSWS.

This paper documents a general methodology for classifying and quantifying the local pressure losses in VSWS using available empirical models. A thorough review of the available empirical/analytical models, developed primarily for industrial applications and the process industry, revealed several models of practical relevance. The advantages and disadvantages of these models were reviewed with emphasis on their appropriateness for building science applications.

In general, simple models, such as the crack flow method and power law approach, are user friendly, but they cannot be applied

directly to the whole range of expected airflows and geometries in VSWS. Both models are insensitive to the variation in local resistance coefficients for different flow regimes characterized by the Reynolds numbers of the flow through the vent.

More complex models such as the airflow through gaps, as well as Idelchik's model for any-edge orifice in the laminar and transitional flow, appear to be promising alternatives. The complex models are defined by set of empirical algebraic equations accompanied by detailed, calibrated tables for local resistance coefficients. The implementation of these models does not require highly skilled professionals and can easily be automated. However, if the calculation requires the determination of the available flow rate in VSWS based on the driving pressure differential at the inlet and outlet vent openings, iterative procedures for solving the set of algebraic equations embedded in the complex models are inevitable. Solving the problem may be a cumbersome task for engineers, and some advanced mathematical and programming skills might be necessary to implement the proposed models efficiently.

Performed laboratory experiments and field studies of the VSWS within the framework of ASHRAE Research Project RP-1091 provide an excellent opportunity to validate proposed empirical/analytical models. The intent of the authors is to publish the results of this analysis in another paper (Part 2) considering it as a logical extension to the present work.

Acknowledgments

The ASHRAE Research Project RP-1091 "Characterization of Ventilation Airflow in Screened Wall Systems" was funded by ASHRAE.

References

[1] ASHRAE. Handbook of fundamentals. Atlanta, GA: American Society of Heating, Refrigeration, and Air Conditioning Engineers; 2009.
[2] ASHRAE. Duct fitting loss coefficient tables. Atlanta, GA: American Society of Heating, Refrigeration, and Air Conditioning Engineers; 1997.
[3] Idelchik IE. Handbook of hydraulic resistance. 3rd ed. Boca Raton: CRC Press; 1994.
[4] Blevins RD. Applied fluid dynamics handbook. New York: Van Nostrand Reinhold Company Inc.; 1984.
[5] Straube J, Burnett E. Vents, ventilation drying and pressure moderation – report. University of Waterloo. Building Engineering Group; 1995.
[6] Allard F. Natural ventilation in buildings – a design handbook. London: James & James; 1998.
[7] Awbi HB. Ventilation of buildings. 1st ed. London: E & FN Spon; 1991.
[8] Hagentoft CE. Introduction to building physics. Lund, Sweden: Studentlitteratur; 2001.
[9] Baker PH, Sharples S, Ward IC. Air flow through cracks. Build Environ 1987; 22(4):293–303.
[10] Dolls WS, Walton GN. CONTAMW 2.0 user manual (NISTIR 6921). National Institute of Standards and Technology (NIST). Building and Fire Research Laboratory; 2002.
[11] Clarke JA. Energy simulation in building design. Bristol and Boston: Adam Hilger Ltd.; 1985.
[12] Etheridge DW. Crack flow equations and scale effect. Build Environ 1977;12: 181–91.
[13] Etheridge DW, Sandberg M. Building ventilation – theory and measurement. Chichester, England: John & Wiley Sons; 1996.
[14] Sherman M. A power law formulation of laminar flow in short pipes. J Fluid Eng 1992;114:601–5.
[15] Cole JT, Zawacki TS, Elkins RH, Zimmer JW, Macriss RA. Application of generalized model of air infiltration to existing homes. ASHRAE Trans 1980; 86(2):765–77.
[16] Sherman MH, Grimsrud DT. Infiltration–pressurization correlation: simplified physical modeling. ASHRAE Trans 1980;86(2):778–807.
[17] Feustel HE, Dieris J. A survey of airflow models for multizone structures. Energy Build 1992;18:79–100.
[18] Hens H. Bouwfysica 1: Warmte- en massatransport. 3rd ed. Belgium: ACCO Leuven; 1992.
[19] Liersch KW. Belüftete dach- und wandkonstruktionen: Bauphysikalische grundlagen des wärme- und feuchteschutzes. Wiesbaden/Berlin: Bauverlag; 1981.
[20] Batchelor GK. Introduction to fluid dynamics. Cambridge: Cambridge University Press; 1967.
[21] IEA. Annex 20: Air flow patterns within buildings – air flow through large openings in buildings (subtask – 2: air flows between zones). In: van der Maas J, editor. CH 1015 Lausanne, Switzerland: LESO-PB, EPFL; 1992.

Legend

A: Cross-section area of the cavity gap (m^2)
a: constant (−)
b: coefficient, gap width, thickness of the opening in cladding wall (−), (m)
C: constant, local pressure loss coefficient, contraction or discharge coefficient (−)
D: diameter (m)
F: Cross-sectional area (m^2)
f: friction coefficient (−)
H: height of the ventilated chamber (m)
K: local pressure loss coefficient (−)
k: constant (−)
L: crack length, gap length (m)
l: orifice length (m)
n: exponent (−)
p: pressure (Pa)
Q: volumetric flow rate of air (m^3/s)
Re: Reynolds number (−)
S: airflow resistance coefficient [$Pa/(m^3/s)$], [$Pa/(m^3/s)^2$]
W: width of the ventilated chamber, width of the crack (m)
w: velocity (m/s)
Greek symbols:
α: constant (−)
β: coefficient, constant (−)
Δ: pressure drop
δ: wall cavity depth (m)
φ: coefficient (−)
ν: kinematic viscosity of the air (m^2/s)
ρ: air density (kg/m^3)
τ: coefficient (−)
ζ: local pressure loss coefficient (−)
Superscripts and subscripts:
∞: outdoor air
0: orifice
1: inlet section
2: outlet section
bot: bottom vent opening
C: contraction
ch: change of stream direction
cr: crack
D: discharge
e: entrance, exit
fr: friction
g: gap
h: hydraulic
op: opening
top: top vent opening
wall: wall surface